Desalination and Water Treatment
www.deswater.com

doi: 10.5004/dwt.2022.28138

252 (2022) 108–125
March

Synthesis of ZnO-TiO_2/activated carbon (ACαZnO/TiO_2) nanoparticles and its application in adsorption of arsenic from aqueous media: study of isotherm and adsorption kinetics and optimization using response surface methodology-central composite design

Nastuna Ghanbari Sagharloo, Mohammad Rabani*, Lida Salimi*, Hossein Ghafourian, Seyed Mohammad Taghi Sadatipour

Department of Environmental Engineering, Tehran North Branch, Islamic Azad University, Tehran, Iran, Tel. 09121302285; email: m_rabani@yahoo.com (M. Rabani), Tel. 09123267297; email: l_salimi@iau-tnb.ac.ir (L. Salimi), Tel. +989113677496; email: ghanbarinastuna@gmail.com (N. Ghanbari Sagharloo), Tel. 09121098062; email: h_ghafourian@iau-tnb.ac.ir (H. Ghafourian), Tel. 09121908960; email: smt_sadatipour@iau-tnb.ac.ir (S.M.T. Sadatipour)

Received 1 October 2021; Accepted 5 January 2022

ABSTRACT

Arsenic contaminated water is a serious threat to human health. Therefore, the aim of this study was to use a new method of stabilization of ZnO/TiO_2 on activated carbon (I ZnO/TiO_2) for the effective removal of arsenic from aqueous solutions. In this experimental study, a container with a useful volume of 3.14 L (height of 40 cm and diameter of 10 cm) was used. For this purpose, four main factors including pH (3–11), nanosorbent dose (1–3 g/L), initial arsenic concentration (1–10 mg/L), and reaction time (30–300 min) as effective factors in the arsenic removal efficiency. The results showed that arsenic adsorption increased with increasing contact time, adsorbent dose, and decreasing pH and arsenic concentration. A quadratic model was selected to estimate the removal of arsenic by the adsorption process with the modified adsorbent under study. The linear regression coefficient (R^2) between experiments and different response values in the model for arsenic was >0.99. The optimal value for the studied variables was obtained for pH of 6.75, arsenic concentration of 9.76 mg/L, reaction time of 287.62 min, and nanosorbent dosage of 2.45 g/L. The maximum arsenic adsorption capacity under optimal conditions was predicted to be 4.53 mg/g. The results showed that the studied adsorbent for arsenic removal follows the Langmuir isotherm and quadratic kinetics ($R^2 > 0.99$). The results of this study showed that the adsorption process using nano-photocatalytic adsorbents of TiO_2 and ZnO has relatively high efficiency in arsenic adsorption and can be used as a suitable complementary treatment method for water and wastewater containing carcinogenic heavy metals such as arsenic.

Keywords: Adsorption process; Arsenic; ACαZnO/TiO_2 nanoparticles; Central composite design; Optimization; Aqueous solutions

1. Introduction

Increasing the concentration of heavy metals in aquatic environments is a serious problem that threatens surface and groundwater resources [1–3]. Heavy metals due to natural interactions or due to human presence in the environment and discharge of contaminated effluents, mining, or excessive use of water resources and as a result, increasing the concentration of these materials leads to non-compliance of water properties with the declared standards, and

* Corresponding authors.

therefore, it cannot be used without treatment and removal of heavy metals [4–7]. Heavy metals and metal complexes in aqueous media have different functions, which are dependent on the environmental conditions, the colloidal state of water, pH, ionic concentration of the solution, the colloidal concentration of metals, and the competition of metal cations. Even the presence of organic and inorganic ligands plays a role in it [8–10]. The most important issue about the pollution of aquatic environments with heavy metals is the excessive entry into the human body through water, food, and air. Lack of metabolism of heavy metals in the body causes accumulation and deposition in adipose tissue or muscle, bones, and joints, which generally causes neurological disorders (Parkinson's, Alzheimer's, depression), various cancers, brain deficiency, and hormonal imbalance [11]. Living organisms need very small amounts of heavy metals to continue growing and surviving, which are called trace elements, such as iron, cobalt, copper, magnesium, molybdenum, vanadium, strontium, and zinc, and other heavy metals such as mercury, lead, and cadmium are not vital elements and do not have beneficial effects on the life of body organisms [12–14]. Arsenic sources vary in the environment; however, minerals, rocks, sediments, soils, fossil fuels, volcanic areas, and the atmosphere are generally arsenic sources. In natural waters, arsenic is often inorganic in the form of trivalent (arsenite) or pentavalent (arsenate) oxyanions. Organic forms of arsenic may form in surface waters as a result of biological activity but are not quantitatively significant [15]. Organic arsenic is often found in water polluted by industrial effluents. The concentration of arsenic in groundwater in most countries is less than 10 μg/L and is sometimes substantially much lower. However, some countries show arsenic levels in the range of 0.5–500 μg/L. This concentration has occurred due to natural conditions and factors [16]. Humans can be exposed to arsenic in a variety of ways. Waters from wells drilled in arsenic-rich soil layers, wells contaminated with industrial or agricultural wastes, contaminated dust, food contaminated with arsenic pesticides or grown with arsenic-contaminated water or arsenic-rich soil can expose humans to arsenic. For most people, dietary sources are the source of arsenic intake, and lower amounts are received from the climate [17]. The importance of arsenic is due to the disruption of DNA and RNA synthesis, which results in cancer. Increased births of exceptional children, low birth weight, abnormal births, and stillbirths are also observed due to the introduction of arsenic compounds. Chronic arsenic poisoning occurs after a long period (between 5 and 20 d) of arsenic exposure, which symptoms of acute poisoning, including nausea, gastrointestinal pain, and diarrhea, immediately appear [18,19]. Symptoms of chronic poisoning have been caused by prolonged exposure to arsenic and include weight loss, chronic weakness, arsenicosis, cardiovascular disease, skin ulcers, and skin cancers. Exposure to arsenic, even in small amounts (0.05 mg/L), increases the risk of cancer of the skin, lungs, urinary tract, bladder, and kidneys. It also causes skin changes (causing dark or light spots on the skin). Increasing the thickness or yellow bulge on the skin and adverse effects on the nervous system (tremors and pain in the scalp) are other side effects of arsenic poisoning [20]. Inhalation of arsenic vapors causes respiratory diseases such as bronchitis, laryngitis, and swelling of the mucous membranes. The effect of arsenic on the stomach and intestines has also been seen, the symptoms of which are burning lips, swallowing with pain, thirst and colic, nausea, and diarrhea [21,22]. For this purpose, various methods such as oxidation process [23], coagulation and filtration [24], membrane methods [25], adsorption [26,27], ion exchange [28], and nanoparticle technology [29] have been investigated for arsenic removal. Nanoparticles have many applications in all sciences, and in the treatment industry, they show great flexibility. Nanoparticles that are activated by light, such as high-energy semiconductors, for example, titanium dioxide (TiO_2) and zinc oxide (ZnO) have been consistently studied for their ability to remove and treat contaminants, and these materials are readily available, inexpensive, and of low toxicity [30–35]. Vaiano et al. [36] conducted a study for enhanced photocatalytic oxidation of arsenite to arsenate in water solutions by a new catalyst based on MoO_x supported on TiO_2. The results showed that TiO_2 alone is not able to oxidize all As(III) present in solution, while the complete conversion of As(III) to As(V) was achieved in the presence of MoO_x/TiO_2 catalyst. In another study, Gholami et al. [37] conducted research on the application of ZnO/TiO_2 nanocomposite for photocatalysis of a herbicide (Bentazon). The results showed that the greatest removal of herbicide was observed at neutral pH due to photocorrosion of ZnO on composite in acidic and basic conditions.

In recent decades, the application of nanotechnology in the removal of various contaminants such as dyes due to their ease and economic use compared to physicochemical and biological methods has been further developed. Toxicity, stability, and concentration of pollutants have significant environmental, economic, and health effects. One of the basic solutions to solve these challenges is the use of technologies that have low investment and operation costs and are very small in size but have a high capacity [31,38,39]. Therefore, this study was performed with the aim of adsorption of arsenic using the method of stabilization of ZnO/TiO_2 nanoparticles on activated carbon (ACαZnO/TiO_2) from aqueous media.

2. Materials and methods

2.1. Materials and equipment

In the present study, arsenic trioxide (As_2O_3), triethanolamine ($C_6H_{15}NO_3$), zinc acetate dihydrate ($Zn(CH_3COO)_2{\cdot}2H_2O$), titanium butoxide ($Ti(OBu)_4$), and granular activated carbon (GAC) were prepared from Sigma-Aldrich. Nitric acid (HNO_3), zinc oxide (ZnO), hydrochloric acid (HCl), and titanium dioxide (TiO_2) were also purchased from Merck (Germany). HACH model sension1 (USA) pH meter was used to adjust the pH. For the evaluation of ZnO/TiO_2 AC nanosorbent microstructures, the Field-Emission Scanning Electron Microscope FE-SEM model scanning electron microscope (SEM) was used. For determination of phases and crystallinity of nanosorbent, an X-ray diffraction pattern (XRD) (STADIP model, Germany) was employed, and for determination of ZnO/TiO_2 AC nanosorbent, elemental analysis X-ray energy diffraction (EDX), and EDX-mapping spectroscopy were used.

2.2. Preparation and synthesis of materials

There are various manufacturing methods for the production of TiO_2 and ZnO nanoparticles, including sol-gel, hydrothermal, and co-precipitation; but in this study, because TiO_2 and ZnO nanoparticles are coated on the basis of catalyst (activated carbon), the method of present work, similar to that of catalysts, was impregnation or immersion. For this purpose, first, the activated carbon was thoroughly washed with distilled water and then dried at 50°C for 2 h. The precursors of TiO_2 and ZnO catalysts were prepared in a separate container. In the next step, by obtaining the stoichiometric ratio and calculating the molecular weight of titanium butoxide and zinc acetate, the amount of precursor removal from the main substance is calculated so that 20 mL of titanium butoxide and 12.6 g of zinc acetate are dissolved in 100 mL of ethanol and stirred with a magnet at 50°C for 1 h to dissolve completely. The dried catalyst base (activated carbon) was poured into a 250 mL beaker, and carbon was stirred with a magnet, then 100 mL of catalytic precursors were added through a burette to a beaker containing activated carbon for 20 min. Stirring was then continued for 2 h at 60°C until the ethanol solvent was completely evaporated and the carbon was completely dried, and finally, the dried carbon was placed at 400°C for 2 h for the calcination process. There are various manufacturing methods for the production of TiO_2 and ZnO nanoparticles, including sol-gel, hydrothermal, and co-precipitation; but in this study, because TiO_2 and ZnO nanoparticles are coated on the basis of catalyst (activated carbon), the method of present work, similar to that of catalysts, was impregnation or immersion. For this purpose, first, the activated carbon was thoroughly washed with distilled water and then dried at 50°C for 2 h. The precursors of TiO_2 and ZnO catalysts were prepared in a separate container. In the next step, by obtaining the stoichiometric ratio and calculating the molecular weight of titanium butoxide and zinc acetate, the amount of precursor removal from the main substance is calculated so that 20 mL of titanium butoxide and 12.6 g of zinc acetate are dissolved in 100 mL of ethanol and stirred with a magnet at 50°C for 1 h to dissolve completely. The dried catalyst base (activated carbon) was poured into a 250 mL beaker. The carbon was stirred with a magnet, and 100 mL of catalytic precursors were then added through a burette to a beaker containing activated carbon for 20 min. Stirring was then continued for 2 h at 60°C until the ethanol solvent was completely evaporated and the carbon was completely dried, and finally, the dried carbon was placed at 400°C for 2 h for the calcination process.

2.3. Design and construction of studied pilot

The present study was performed on a laboratory scale and discontinuously in a container (made of Pyrex glass) with a useful volume of 3.14 L and a height of 40 cm, and a diameter of 10 cm. The actual shape and complete specifications of the reactor used in this study are presented in Fig. 1. The studied reactor consisted of a lamp chamber made of quartz tube with a height of 40 cm and a diameter of 3.6 cm and also had a UV lamp made of a quartz with a height of 25 cm and a diameter of 3 cm. The whole reactor was controlled by a control panel mounted next to the reactor.

2.4. Design and optimization of experiments by central composite design-response surface methodology method

Response surface methodology (RSM) is a set of statistical techniques used to optimize processes in which the desired response is affected by a number of variables. This method creates a polynomial from the samples and data obtained and explains the relationships between these data. Now, to analyze and create polynomials in this method, different statistical models such as central composite design (CCD), Box–Behnken, etc. are used [40–43]. In the present study, statistical design of experiments and data analysis was performed using CCD by Design-Expert statistical software (version 11). The design of experiments with the CCD approach is known as the strongest and most effective subset of RSM. This approach has also been reported as a very effective method in modeling and optimizing wastewater treatment processes. According to Table 1, the domain and levels of variables (nanosorbent dose, pH, reaction time, and initial concentration of arsenic) were examined at three levels with codes of +1, 0, and –1 for high, medium, and low values, respectively. Based on CCD, 30 experiments were designed. The laboratory conditions used in this study are shown in Table 2. Data obtained from responses of the RSM model were calculated using analysis of variance (ANOVA)**.** Response variables for arsenic adsorption (response variable, q_e) in the form of the following polynomial regression model [Eq. (1)] were presented as a function of independent variables [44,45]:

$$Y = \beta_0 + \sum_{i=1}^{k} \beta_i X_i + \sum_{i=1}^{k} \beta_{ii} X_i^2 + \sum_{i=1}^{k-1} \sum_{i=i+1}^{k} \beta_{ij} X_i X_j \quad (1)$$

where Y is the response variable for the factor level (arsenic removal efficiency); β_0 is intercept; β is the regression coefficient calculated from the values obtained from Y. Sections of $X_i X_j$ and X_{i2} include criteria for interactive and quadratic interaction, respectively [46,47]. The nominal fit quality of the polynomial equation was evaluated using the obtained coefficients R^2 and the values of R^2 (adjusted-R^2) to measure the suitability of the model. $P < 0.05$ was considered as the appropriate significance. Because the optimal conditions provided by the software are theoretical, the experiments presented were reviewed and compared in terms of operational and practical conditions. Therefore, the optimal operating conditions were studied and tested separately. In this regard, in optimal operating conditions, experiments were performed with three repetitions and the suitability of the model was evaluated. Finally, inductively coupled plasma atomic emission spectrometry (ICP/AES) was used to measure arsenic heavy metal.

2.5. Adsorption isotherm and kinetics studies

The kinetics of adsorption can be described using several models. A simple kinetic model is the pseudo-first-order equation [Eq. (2)] [48,49]:

$$\frac{dq_t}{dt} = K_1 \left(q_e - q_t \right) \quad (2)$$

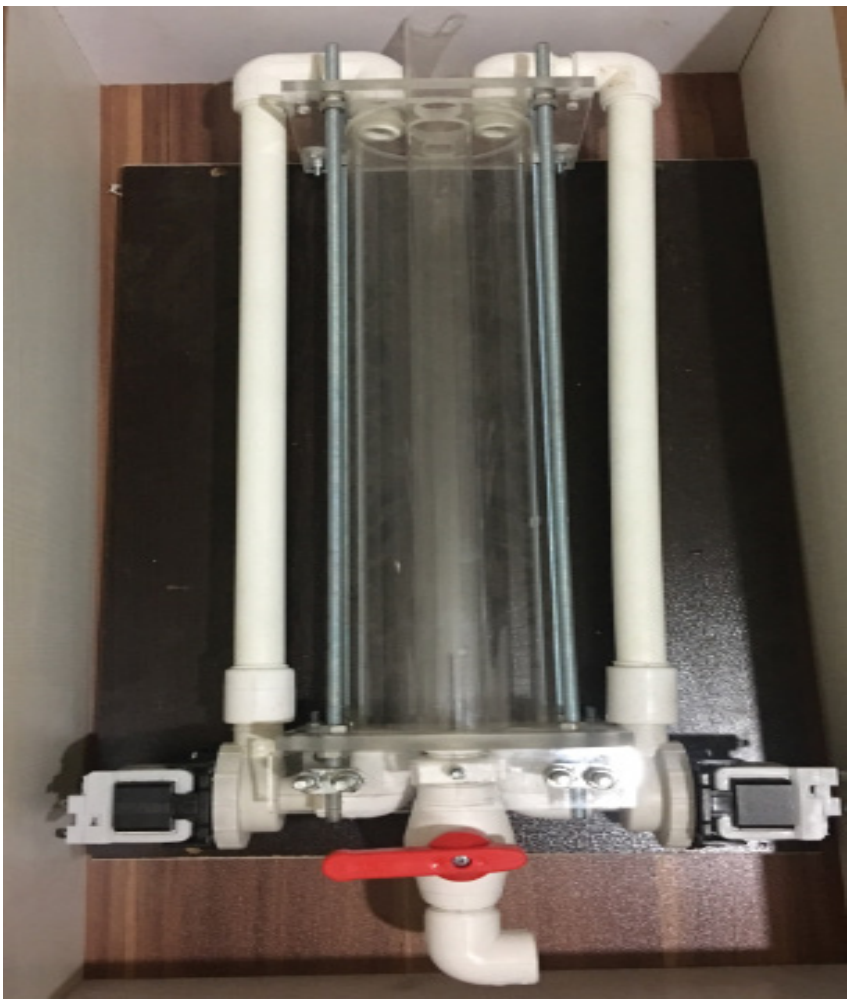

Manufacturer	Height (cm)	Volume	Diameter (cm)	Material	Name
Tehran pyrex	40	3.14	10	Pyrex glass	**Reaction chamber**
Germany	40	0.41	3.6	Quartz tube	**Lamp chamber**
Philips, Germany	25	-	3	Quartz	**UV lamp**
The control panel was manufactured by a manufacturer in Lalehzar Ordered for production (Pak Abnama Engineering Company)					**Electrical control panel** **Adsorbent**

Fig. 1. The actual shape of the pilot examined in this study.

Table 1
Range of experiments and levels of independent variables

	Independent variables	Ranges and levels		
		–1	0	+1
A	Nanosorbent dose, g/L	1	2	3
B	pH	3	7	11
C	Reaction time (T), min	30	165	300
D	Arsenic concentration (C), mg/L	1	5.5	10

After definite integration by applying the initial conditions $q_t = 0$ at $t = 0$ min and $q_t = q_t$ at $t = t$, Eq. (2) becomes Eq. (3) [50]:

$$\log\left(q_e - q_t\right) = \log q_e - \frac{K_1}{2.303}t \tag{3}$$

where q_e and q_t are the amounts of adsorbate adsorbed (mg/g) at equilibrium and at any instant of time t (min), respectively and K_1 is the rate constant for pseudo-first-order adsorption (1/min).

The pseudo-second-order kinetic model based on equilibrium adsorption can be represented in Eq. (4) [51,52]:

$$\frac{t}{q_t} = \frac{1}{K_2 q_e^2} + \frac{t}{q_e} \tag{4}$$

where K_2 is the equilibrium rate constant of pseudo-second-order adsorption (g/mg min).

The adsorption process is always correlated with theoretical equations which can be depicted by isotherm models that are shown by the following equations. Freundlich isotherm is one of these models, which is utilized to portray the adsorption on heterogeneous surfaces. This model can be shown by the following equation [Eq. (5)] [53]:

Table 2
Results of experiments performed for the studied response (arsenic adsorption)

Run	*A*: nanosorbent dosage (g/L)	*B*: pH	*C*: reaction time (min)	*D*: arsenic concentration (mg/L)	q_e (mg/g)	
					Actual value	Predicted value
1	2	7	165	5.5	2.19	2.20
2	1	11	300	10	7.85	7.86
3	1	7	165	5.5	3.09	3.08
4	2	7	30	5.5	1.09	1.08
5	2	7	300	5.5	3.35	3.35
6	3	3	300	10	3.76	3.77
7	1	11	30	1	0.26	0.26
8	3	3	30	10	0.66	0.64
9	3	11	30	1	0.89	0.88
10	1	3	300	1	1.66	1.65
11	1	3	30	10	2.58	2.59
12	1	11	300	1	1.68	1.69
13	3	11	300	1	0.12	0.12
14	2	7	165	5.5	2.25	2.20
15	1	3	300	10	7.88	7.88
16	2	7	165	5.5	2.19	2.20
17	1	11	30	10	2.52	2.51
18	2	7	165	5.5	2.17	2.20
19	3	3	30	1	0.96	0.96
20	3	11	30	10	0.47	0.49
21	3	7	165	5.5	1.34	1.33
22	2	11	165	5.5	2.19	2.18
23	2	3	165	5.5	2.24	2.23
24	3	11	300	10	3.68	3.67
25	2	7	165	1	0.75	0.74
26	2	7	165	10	3.68	3.67
27	3	3	300	1	0.15	0.15
28	2	7	165	5.5	2.20	2.20
29	2	7	165	5.5	2.17	2.20
30	1	3	30	1	0.27	0.27

Std. Dev.	0.0223	R^2	0.9999
Mean	2.21	Adjusted R^2	0.9988
C.V. %	1.01	Predicted R^2	0.9958

$$q_e = KC_e^{1/n} \tag{5}$$

where C_e is the equilibrium concentration of the solution (mg/L), q_e is the amount of adsorbed arsenic per unit of adsorbent mass (mg/g), K is Freundlich constant, and $1/n$ represents the adsorption intensity. The linear form of this isotherm model is as follows in Eq. (6) [54]:

$$\log q_e = \log K_F + \frac{1}{n}\log C_e \tag{6}$$

The curve obtained from the $\log q_e$ vs. $\log C_e$ can help to calculate the parameters of Freundlich isotherms.

Langmuir isotherm model describes the systems that are having simple monolayer adsorption onto the adsorbent surface. This model has supposed that the adsorption takes place at specific adsorption sites. Therefore, Langmuir isotherm can be defined according to Eq. (7) [55]:

$$\frac{C_e}{q_e} = \frac{1}{q_m b} + \frac{C_e}{q_m} \tag{7}$$

where C_e is the equilibrium concentration of the arsenic in solution (mg/L), q_e is the adsorption capacity at equilibrium (mg/g), b (L/mg) is the Langmuir constants, related to the binding constant, and q_m (mg/g) is the maximum adsorption capacity.

3. Results and discussion

3.1. Determination of nanosorbent characteristics

Scanning electron microscopy can provide various information about the surface layers of matter by generating an electron beam and shining it on the sample surface and scanning the return rays. Therefore, in this research, the scanning electron microscopy (SEM) technique was used to evaluate the nanostructures of I ZnO/TiO_2 AC nanosorbent at different magnifications (500 nm and 1, 20, 10, and 50 μm), which are shown in Fig. 2. According to Fig. 2, ZnO/TiO_2 nanoparticles are regularly dispersed in AC. The results also show that ZnO and TiO_2 cover most of the AC surface and increase the catalytic activity of I ZnO/TiO_2 AC due to good interaction with UV rays. The black-and-white section of the image shows morphology, cast, and particle size, as well as the general state of in vitro synthesis of I ZnO/TiO_2 AC. This clearly shows that I ZnO/TiO_2 AC has different morphology, shape, and size, which creates a heterogeneous photocatalytic adsorbent. In addition, according to the shape, the particle size is between 57.92 to 63.33 nm, so the particle structure is confirmed as a nanoscale (<100 nm). Elemental analysis of ZnO/TiO_2 AC nanosorbent was performed using X-ray energy diffraction (EDX) and EDX-Mapping spectroscopy, and the results are presented in Figs. 3a and b. According to the results, the main elemental compounds of C, O, Ti, Cr, and Zn were obtained with weight percentages of 10.65%, 21.12%, 5.79%, 6.7%, and 55.73%, respectively.

X-ray diffraction test is a non-experimental method that provides comprehensive information about the chemical composition and crystal structure of natural and industrial materials. Each crystal material has its own unique X-ray diffraction pattern that may be used as a fingerprint for identification. The most widespread use of XRD is in the identification of crystalline compounds based on their diffraction pattern. Therefore, in the present study, the X-ray diffraction (XRD) pattern of powder samples was used

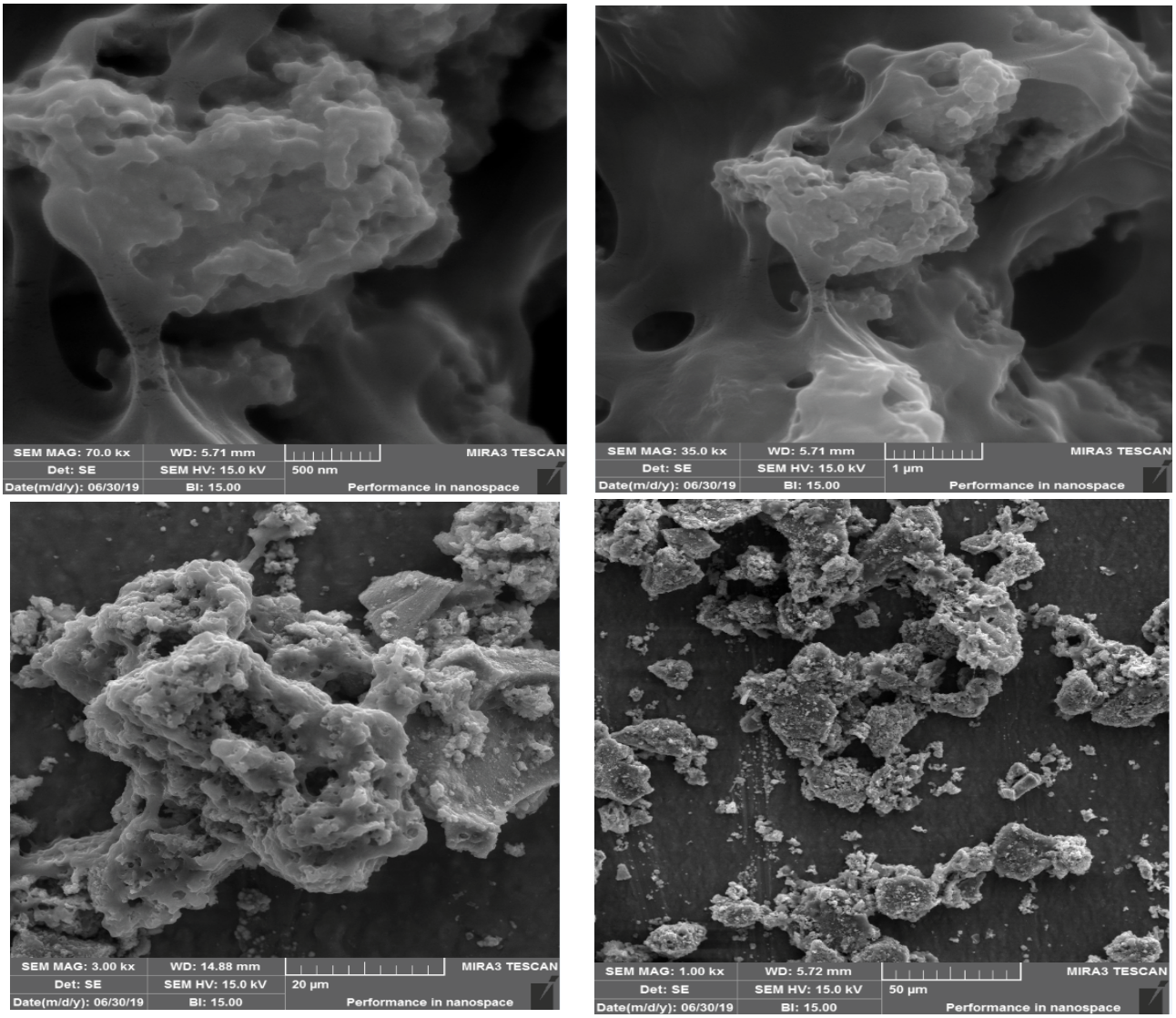

Fig. 2. SEM images of I ZnO/TiO_2 AC nanosorbent with different magnifications.

to determine the phases and crystallinity of I ZnO/TiO_2 AC nanosorbents (Fig. 3c). According to the results, the peaks and phases of the main rutile observed at 2θ for the examined I ZnO/TiO_2 AC nanosorbent were 27.44° (110), 36.07° (011), 39.20° (020), 41.24° (111), 44.05° (120), 54.32° (121), 56.64° (220), 62.72° (002), 64.06° (130), 69.01° (031), and 69.78° (112). Also, the main peaks of the anatase phase were obtained at 2θ including 25.31° (011), 37.75° (004), 48.06° (020), 53.86° (015), 55.08° (121). Considering the XRD pattern, it is quite clear that the main peaks at 2θ are 31.80° (010), 34.46° (002), 36.29° (011), 47.57° (012), 56.62° (110), 62.88° (013), 67.96° (112) and 69.10° (021), which

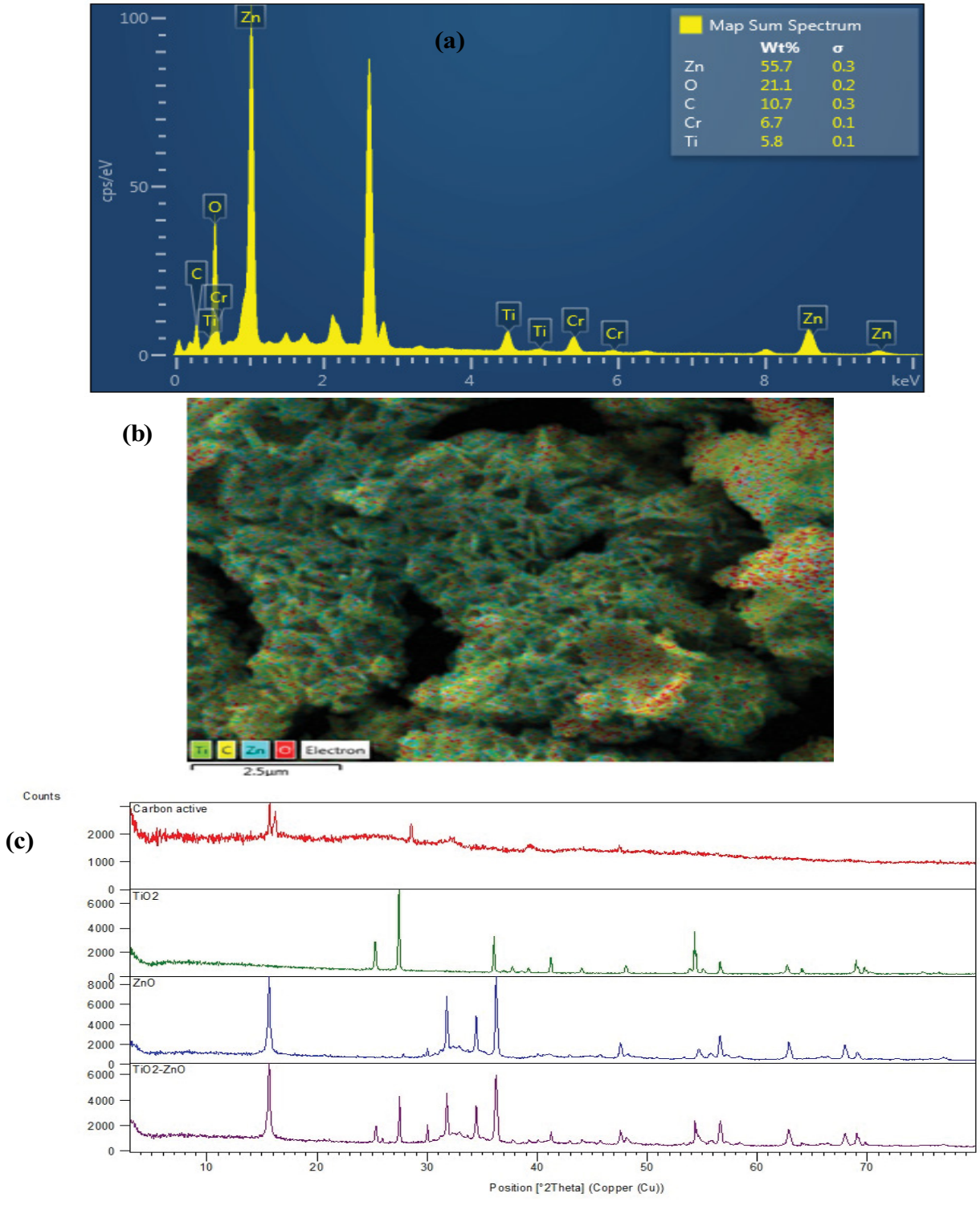

Fig. 3. (a) EDX image, (b) EDX-mapping image, and (c) XRD spectrum image of the I ZnO/TiO_2 AC nanosorbent.

confirm the presence of ZnO on the prepared adsorbent. The above facts show that the synthesized I ZnO/TiO_2 AC nanosorbents contain standard ZnO and TiO_2.

3.2. Modeling the adsorption process by RSM-CCD method

Central composite design (CCD) was used to find the relationship between process responses and variables. In this study, reaction time, pH, nanosorbent dose, and arsenic concentration were considered as variables, and the amount of arsenic adsorption was considered as the response. In the central composite design used in this study, the total number of experiments was 30 for arsenic adsorption by ZnO/TiO_2 AC nanosorbent. Three levels of +1, zero, and –1 were considered for high, medium, and low values for model fit, respectively. Table 2 presents the test steps, along with the results obtained at each test step.

According to the results presented in Table 3, it is clear that the quadratic model is the most suitable model to describe the adsorption of arsenic from aqueous solutions using titanium dioxide (TiO_2) and zinc oxide (ZnO) nano-photocatalytic adsorbents. Considering the results of Table 3, it is clear that the quadratic model has the highest values of adjusted R^2 (R^2-adj.) and R^2. Therefore, the model was selected for analysis. The overall prediction performance of the model is defined by the coefficient of certainty R^2. In this study, the relatively high value of R^2 (0.9999) indicates a good correlation between the predicted values of the model and the actual values. However, the value of R^2 must be consistent with (close to) R^2-adj. When the two values are very different, it is possible that non-significant expressions are included in the model (146). In the present study, the value of R^2-adj. (0.9958) is very close to the value of R^2. The results of ANOVA analysis with *F*-values and *P*-values of each model expression for the nanosorbent are presented in Table 3. In the ANOVA table, coefficients with *P*-values greater than 0.1 are considered statistically insignificant and are excluded from the quadratic equations. In ANOVA statistical analysis, a significant degree of *P*-value is shown to determine the significance of the response model. *P*-values (0.0001) of arsenic adsorption indicate that the sentences in the studied models are significant ($P < 0.05$). Regarding the significance of the model, as can be interpreted from the above table, the *P*-value is less than 0.05, which means that the model is significant at confidence intervals of 5% (Table 3). Accuracy measurement is an indicator for determining the amount of error in experiments, and the ratio greater than 4 is a desirable value [56]. In the experiments performed in this study, the values of accuracy (491.9232) are significantly greater than 4 (Table 2).

The final model equation is presented to predict the process response in Eq. (8). In this equation, *A*, *B*, *C*, and *D* are the four independent variables in this study, which are defined in Table 2–4.

Table 3
Analysis of variance (ANOVA) for the proposed model for arsenic adsorption

Source	Sum of squares	df	Mean square	*F*-value	*P*-value	
Model	102.63	14	7.33	14,730.84	<0.0001	Significant
A-D	0.0782	1	0.0782	157.15	<0.0001	
B-pH	0.0120	1	0.0120	24.06	0.0002	
C-T	0.1144	1	0.1144	229.91	<0.0001	
D-C	0.0717	1	0.0717	144.07	<0.0001	
AB	0.0053	1	0.0053	10.56	0.0054	
AC	4.74	1	4.74	9,528.05	<0.0001	
AD	6.90	1	6.90	13,873.09	<0.0001	
BC	0.0028	1	0.0028	5.54	0.0327	
BD	0.0046	1	0.0046	9.16	0.0085	
CD	15.43	1	15.43	30,997.04	<0.0001	
A^2	1.994E-06	1	1.994E-06	0.0040	0.9504	
B^2	1.994E-06	1	1.994E-06	0.0040	0.9504	
C^2	0.0001	1	0.0001	0.1798	0.6775	
D^2	1.994E-06	1	1.994E-06	0.0040	0.9504	
Residual	0.0075	15	0.0005			
Lack of fit	0.0031	10	0.0003	0.3580	0.9216	Not significant
Pure error	0.0044	5	0.0009			
Corr. total	102.64	29				

Source	Sequential *P*-value	Lack of fit *P*-value	Adjusted R^2	Predicted R^2	
Linear	<0.0001	<0.0001	0.6545	0.5750	
2FI	0.9673	<0.0001	0.5743	0.4303	
Quadratic	<0.0001	0.1261	0.9975	0.9938	Suggested
Cubic	0.7742	0.0293	0.9967	0.9227	Aliased

Table 4
Comparison of the adsorption capacity of different adsorbents for arsenic adsorption

Adsorbent	Maximum adsorption capacity (q_{max}) (mg/g)	Adsorption isotherm	References
Polythiophene/Fe_2O_3 nanocomposites	42.81	Langmuir	[63]
Adsorption process	0.108	Langmuir	[74]
Adsorption process (BCMDS-YD)	4.56	Langmuir	[79]
Adsorption process	6.46	Langmuir	[77]
ACαZnO/TiO_2 nanoparticles	4.53	Langmuir	In study

$$q_e = 2.75 - 0.89A - 0.05B + 1.10C + 1.49D - 0.049AB - 0.576AC - 0.624AD - 0.027BC - 0.051BD + 1.00CD + 0.446A^2 - 0.374B^2 + 0.618C^2 + 0.314D^2 \quad (8)$$

3.3. Adequacy of the model

The first test, examination of the graph of the normal function of the residuals is shown in Fig. 3a. The difference between the values obtained from the experiment and the values fitted by the model is called the residual. The points obtained from the experiment should be placed on a straight line to indicate the normality of the data; this straight line is usually given on the basis of theoretical observation and preferably with emphasis on the central points to the end [57]. The points are approximately along a straight line, so it can be intuitively concluded that the residual has a normal distribution. Fig. 3a shows that almost all data points are distributed on a straight central line, indicating a normal distribution of data. Fig. 3b shows a graph of the residual values in front of the test number. The error diagram according to the order of the experiment shows the hidden errors and affective on the response. Normally, this chart should follow a random pattern. The existence of a specific trend in this diagram shows that a time-related factor affects the response, and to fix this defect, the experiments should be performed in random order or should be blocked. Fig. 3b shows that the data are randomly scattered, and none of the data deviates from the standard deviation. Thus, it can be concluded that the quadratic model presented in Table 3 is significant and adequate. How the studentized residual changes vs. the fitted (predicted) values is shown in Fig. 3c. In this diagram, the points must be randomly distributed; as it can be seen, the points follow a specific pattern of random scattering. In Fig. 3c, the residual changes do not follow a specific trend, which indicates that the variance is constant. Figs. 3b and c show that all residuals are randomly scattered within the standard deviation range, confirming that none of the experiments need to be repeated.

Box-Cox chart is a tool that helps to determine the most appropriate conversion power of response data [58]. The lowest point in Fig. 4d represents the value of λ that results in the smallest sum of squares of residuals in the model. The potential for improvement is maximum when the range of maximum to minimum response values is greater than 3. Currently, the difference between the maximum and minimum values is less than 3, and therefore there is no need to convert. In Fig. 3d, the lowest point in the Box–Cox scheme (best $\lambda = 1$) confirms that there is no need to transmit the system response.

3.4. Optimization of the main variables in the arsenic adsorption process

The optimization method available in RSM-CCD in Design-Expert software was used to achieve the highest amount of arsenic adsorption. According to the results presented in Fig. 5, the optimal conditions for the studied parameters were pH = 6.75, arsenic concentration of 9.76 mg/L, reaction time of 287.62 min, and nanosorbent dose of 2.45 g/L. Therefore, this row was selected as the optimal operating conditions. The maximum amount of arsenic adsorption under optimal conditions was predicted to be 4.53 mg/g. Because the optimal conditions provided by the software are theoretical, the experiments presented were examined in terms of operational and application conditions. Therefore, in the optimal conditions designed by the software, the optimal values of which are in accordance with Fig. 5, the maximum amount of arsenic adsorption by the proposed model was predicted to be 4.53 mg/g. Then, the optimal experiment was performed with three repetitions according to the value of the mentioned parameters. In practice, the amount of arsenic adsorption was 4.38 mg/g. According to the results, it can be inferred that the actual removal of arsenic has an error of 0.15 mg/g compared to the predicted performance, and this small difference indicates the validity of the fitted model. Fig. 6 presents the results of the study of the effect of each factor alone on the removal of arsenic using nano-photocatalytic adsorbents of titanium dioxide (TiO_2) and zinc oxide (ZnO) under optimal operating conditions.

3.5. Effect of effective parameters on the arsenic adsorption process

Reducing the number of experiments and examining the interaction between parameters, analyzing the results of experiments is an effective method in optimizing various processes, including adsorption processes. Response surface is a powerful statistical tool for designing and analyzing test results, simulating the effect of effective factors on each other, and finding optimal conditions [59]. In classical multivariate optimization experiments, the studied variables are optimized separately, and during optimization of one variable, the other variables are considered constant. In this case, the effect of variables on each other cannot be determined [42,60,61]. In order to investigate the effect of

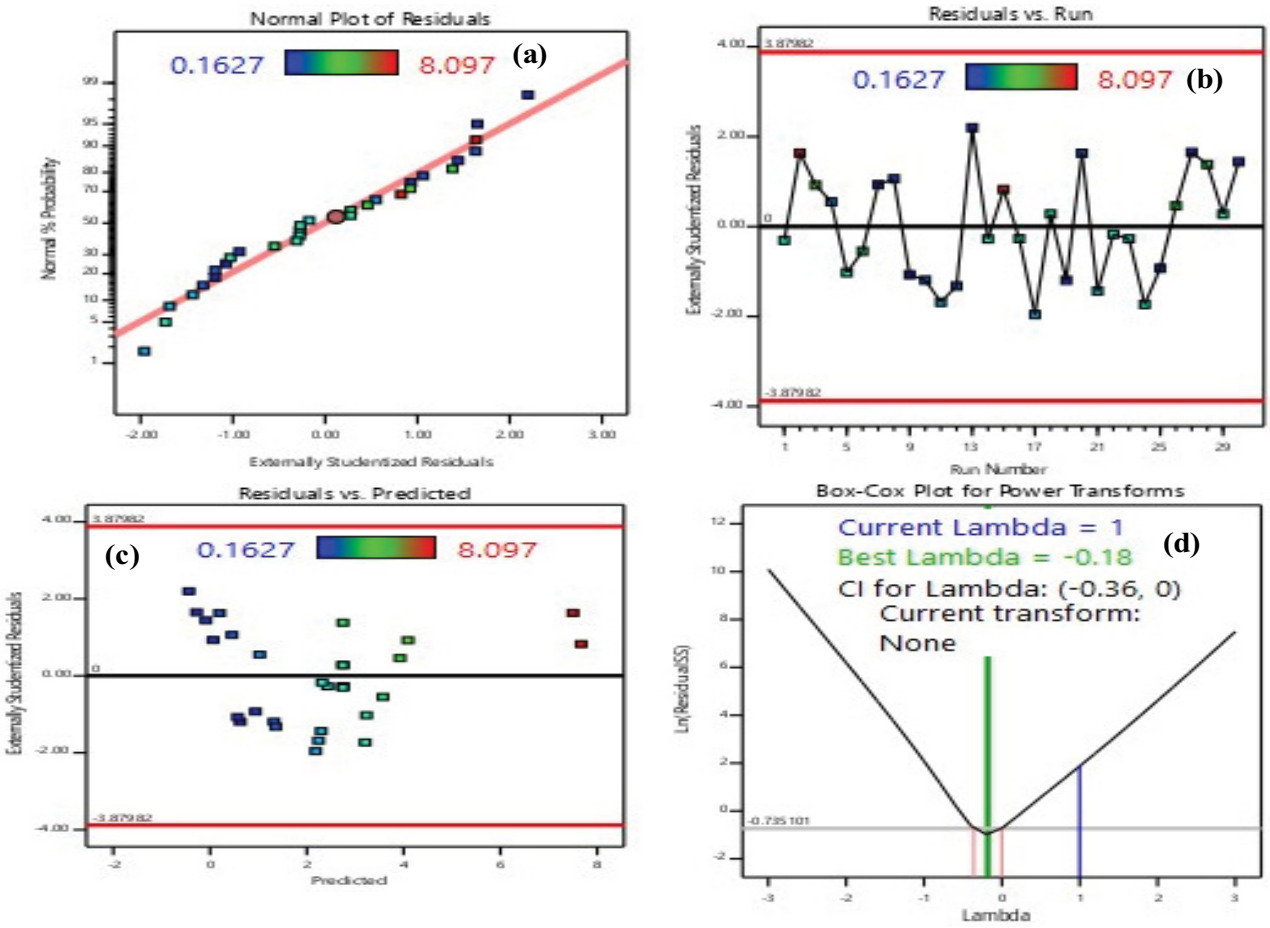

Fig. 4. (a) Distribution of residuals, (b) Graph of residual values vs. predicted values, (c) graph of residual values vs. test number, and (d) Cox–Box diagram of the output of the RSM method for arsenic ion adsorption examined by nanosorbents.

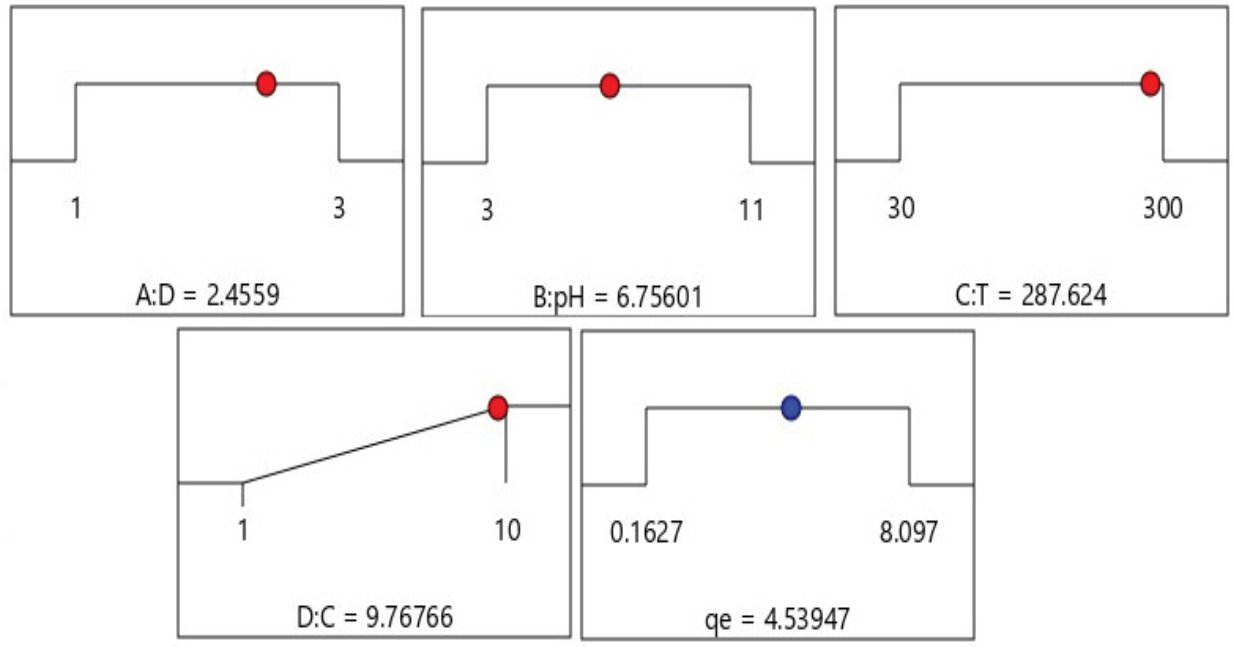

Fig. 5. Diagram of optimal conditions for arsenic adsorption in the process under study.

each variable and the interaction or dual effects of the variables on the response generated by the model, three-dimensional and counter diagrams based on the polynomial function of the model were prepared using experimental design software. Figs. 6 and 7 show the three-dimensional response surface diagrams related to arsenic removal efficiency as a function of initial pH (3–11), arsenic concentration (10–11 mg/L), nanosorbent dose (1–3 g/L), and the reaction time (30–300 min).

The pH of the solution is one of the factors that affect the efficiency of adsorbents by affecting the tendency of the adsorbent surface to the contaminant. For this purpose, one of the most important parameters in the removal of metal ions in the adsorption process is the initial pH of the solution, which has a great effect on the sites of adsorption of metal ions on the adsorbent surface and the chemical structure of the metal in water. It should be noted that at high pH, OH^- ions in solution form complexes with metal ions, which reduces the percentage of metal ion removal [35]. The pH parameter is directly dependent on the competitiveness of hydrogen ions with adsorbed material ions on the active sites of the adsorbent surface. In general, the effect of pH on the adsorption of heavy metals by adsorbents can be attributed to the separation or non-separation of acidic groups. These groups at pH above pK_a are mainly in the dissociated state and can exchange H^+ with metal ions in the solution [62]. While at low pH, it is not possible to bond with the metal cation due to the lack of separation of these functional groups. In this regard, at this stage of the experiments, the pH parameter was examined in the range of 3–11 to investigate the effect of solution pH on the efficiency of the arsenic adsorption process from aqueous solutions. The results showed that at the beginning of the experiment, with increasing the pH to about 7, the amount of arsenic absorption by the studied process increased, and then with increasing the pH from 7 to 11, the efficiency of arsenic adsorption decreased (Figs. 6 and 7). The results of the present study were consistent with the results of the study of Eisazadeh and Hemati [63]. In the study of Eisazadeh and Hemati [63], the highest arsenic uptake efficiency was obtained at a pH of about 6. Also, in a study conducted by Asgari et al. [64] for removing arsenic from drinking water by the adsorption process, the results showed that the highest arsenic removal efficiency was obtained at a pH of about 6, which is consistent with the results of the present study. Also, the results obtained in this study were similar to the results of Banerjee et al. [65]. The results of Banerjee et al. [65] showed that at pH more than 8.5, the arsenic removal efficiency decreased but at pH less than 7.5, the arsenic removal efficiency increased significantly. As in the present study, the highest arsenic removal efficiency was obtained at a pH of about 7, and at values higher than this pH, the efficiency of arsenic removal decreases. In fact, the competition between the hydroxide ion in the solution and the adsorbent sites for the placement of the arsenic metal ion results in a MOH bond, which results in a stable state in the metal in the solution; this reduces the metal transfer to the adsorbent and reduces the adsorption efficiency [66].

Adsorbent dosage or amount of adsorbent is an important parameter in the rate of metal adsorption by adsorbent [67]. Increasing the amount of adsorbent is one of the effective parameters in increasing the adsorption efficiency because with increasing the amount of adsorbent, the existing surface for adsorption of the adsorbate increases [68]. The results of the effect of adsorbent dose on adsorption capacity show that with increasing adsorbent dose, adsorption capacity decreases, and in contrast, removal efficiency increases (Figs. 6 and 7). Increasing the amount of adsorbent means increasing the adsorbent surface and more access of contaminant molecules to the adsorption points on the

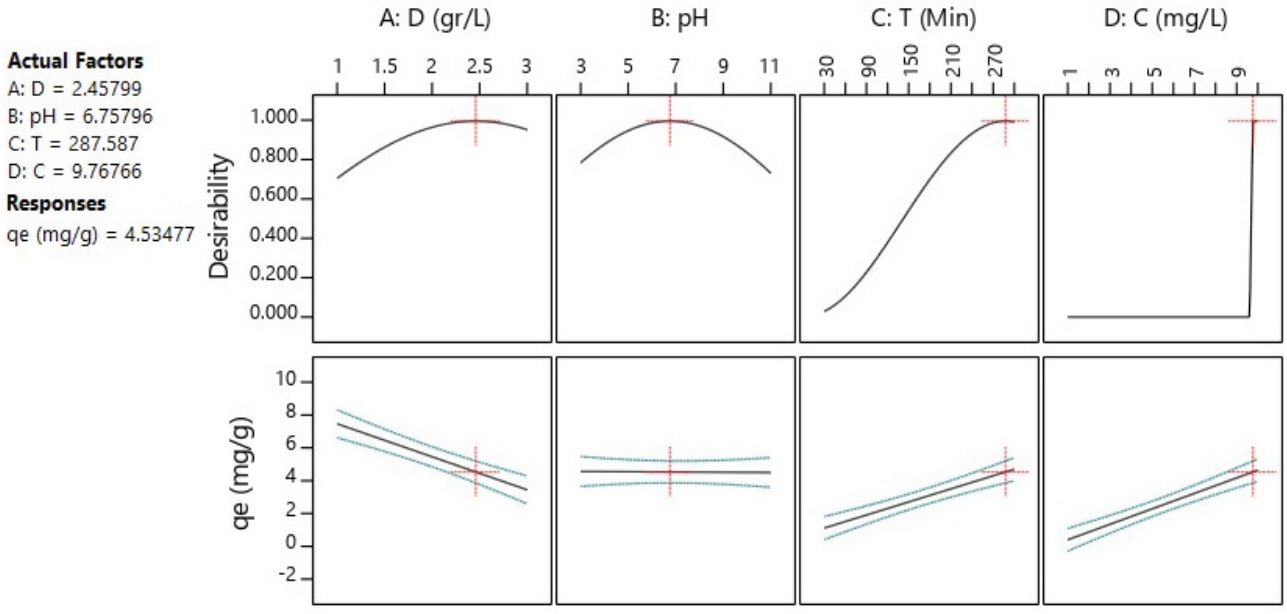

Fig. 6. Diagram of how the effect of the main variables in the optimal operating conditions on the adsorption and desirability of the process.

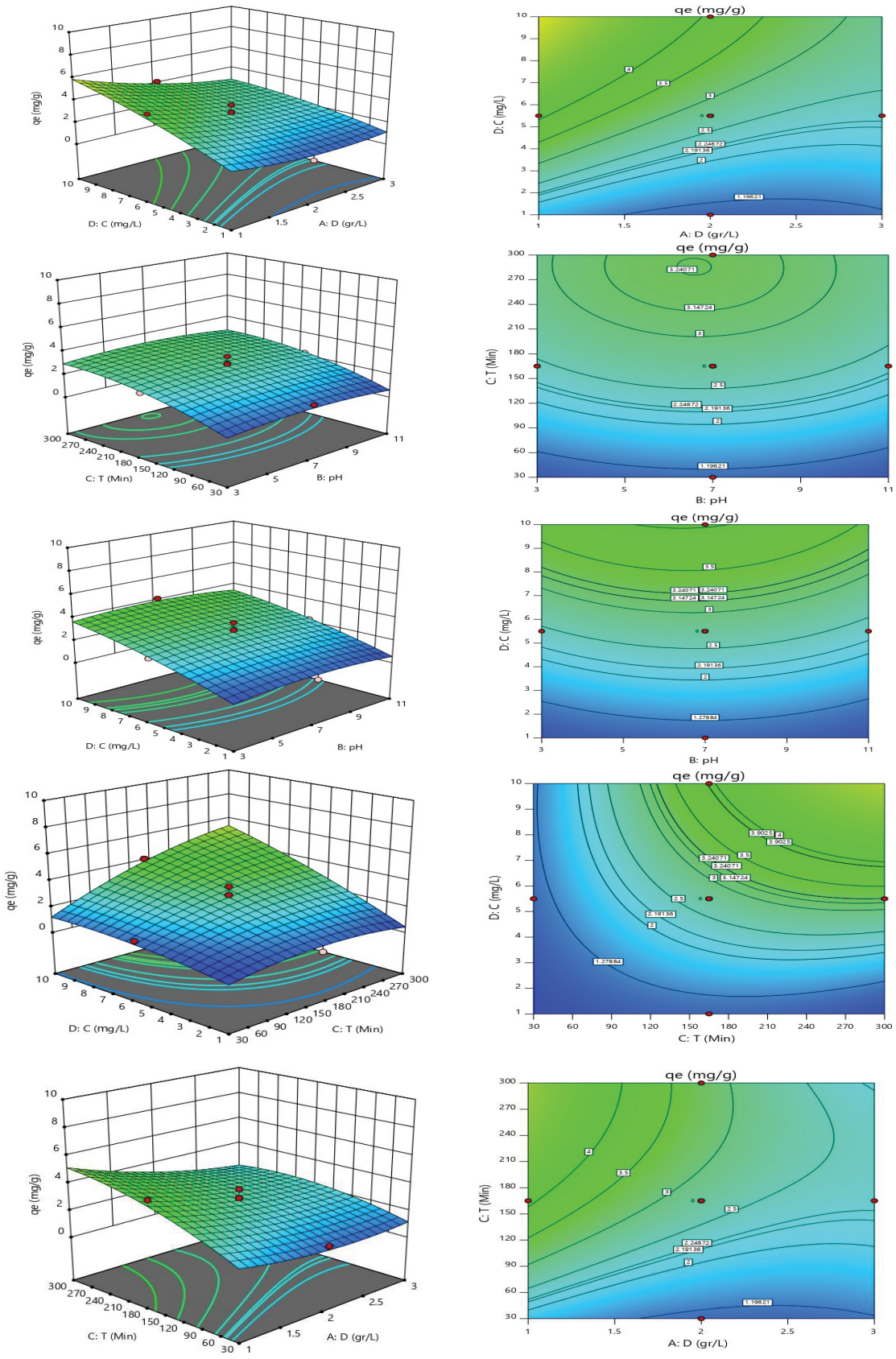

Fig. 7. Three-dimensional and counter diagrams of the interaction of nanoparticle dose and reaction time on the response rate of arsenic removal using nano-photocatalytic adsorbents of titanium dioxide (TiO_2) and zinc oxide (ZnO).

adsorbent surface, which increases the removal percentage. On the other hand, increasing the adsorbent dose means faster adsorption of the contaminant from the solution and decreasing its concentration in the solution. This reduces the number of molecules available to create maximum surface coverage, which reduces the amount of contaminants adsorbed per unit weight of adsorbent. This trend indicates that the adsorbed particles on the adsorbent surface with the molecules remaining in the solution close the internal pores of the adsorbent or cause the adsorption particles to accumulate and coalesce, resulting in a reduction of the active points for adsorption [49]. Adsorption rate is one of the most important factors in the design of adsorption experiments in the laboratory. Consequently, time dependence must be determined in such systems under different process conditions. Since the adsorption processes are of the equilibrium reaction type, so the contact time plays an essential role in the progress of the reaction; also, the reaction proceeds to reach equilibrium. If the adsorbate component easily accesses the adsorption sites of the adsorbent, it needs less contact time to reach the maximum adsorption rate, but if this access is difficult, the contact time should be increased to reach the maximum adsorption [69]. In general, the adsorption process of arsenic metal ions on the adsorbent surface can be divided into two stages, that is, fast and slow. The first step, which is done more quickly, is related to the internal penetration of metal ions.

In the second stage, which occurs at a slower rate, the active binding groups are located in the cell wall of the adsorbent particles. The high initial adsorption rate is due to the surface bonds that these active groups have established with the metal ion. Over time, the decrease in the frequency of active sites decreases the metal adsorption rate. Also, the rapid phase of metal ions by the adsorbents may be due to the presence of many pores and the structure of cavities in the adsorbent, which allows rapid penetration for metal adsorption at binding sites [70]. In this study, it was found that the percentage of arsenic removal by nano-photocatalytic adsorbents of titanium dioxide (TiO_2) and zinc oxide (ZnO) is directly related to the contact time, that is, with increasing the contact time from 30 to 300 min, the amount of arsenic adsorption increases (Figs. 6 and 7). In this process, at the beginning of the adsorption reaction, the removal percentage has increased due to the frequency of adsorption sites and the large difference between the concentration of adsorbate in the solution and its amount at the adsorbent surface [71]. However, this increase has taken on a very gentle slope over time due to the presence of a contaminant layer on the adsorbent surface. It is also difficult to occupy the remaining empty surface areas over time because there is a kind of repulsion between the molecules adsorbed on the adsorbent surface and the molecules in the solution phase. In a study conducted by Mosaferi and Mesdaghinia [72] for arsenic removal in aqueous solutions, the results showed that the adsorption efficiency increased with increasing contact time.

The initial concentration of the pollutant is one of the most important factors affecting the adsorption process; for this purpose, different concentrations of arsenic (1–10 mg/L) were tested in the adsorption process by nano-photocatalytic adsorbents of titanium dioxide (TiO_2) and zinc oxide (ZnO). According to the results, with increasing the initial concentration of arsenic, the amount of adsorbed arsenic also increases, so that it can be said that the removal efficiency of the process is affected by the initial concentration of arsenic. Therefore, in general, at the beginning of the reaction, increasing contaminant concentration was led to increase the efficiency of the process in removing arsenic, but after a while, the efficiency of the process decreased. This phenomenon can be related to the fact that at the beginning and early stages of adsorption, a large number of empty surface sites were available for adsorption. However, the remaining active surface sites decreased over time, and arsenic adsorption subsequently decreased; this may be due to repulsive forces between adsorbed molecules on the surface of the solid adsorbent and the liquid mass [73]. Mentioned results are consistent with the results of the study by Maleki and Eslami [74]. Also, the increase in adsorption capacity with increasing arsenic concentration can be due to the high probability of collision between arsenic ions and the adsorbent surface [74].

3.6. Recyclability performance of the adsorbent for the adsorption of arsenic

The recyclability performance of an adsorbent is an important parameter to evaluate the application of the adsorbent. The re-use of the ACαZnO/TiO_2 nanoparticles adsorbent in the adsorption of arsenic was tested by continuous adsorption experiments under the determined optimum operating parameters by using RSM-CCD. The process mentioned above was repeated ten times under the same conditions to determine the recyclability performance of the adsorbent. The removal efficiency of arsenic ion was consecutively investigated to determine the reusability of the adsorbent (Fig. 8). As shown in Fig. 8, after ten reuses of adsorbent, the removal efficiency of cadmium ion was reduced by only about 2.6%.

3.7. Isotherm and kinetic studies

3.7.1. Isotherm studies

Adsorption isotherms are adsorption properties and equilibrium data that describe how contaminants react with the adsorbent and play an essential role in optimizing adsorbent consumption. Establishing the right relationship for the equilibrium curve and optimizing the design of an adsorption system to remove contaminants is crucial. Equilibrium isotherms of adsorption are presented by plotting the concentration of pollutants in the solid phase vs. the concentration of arsenic in the liquid phase. Langmuir and Freundlich isotherms were used in this study. The results are presented in Fig. 9. The results of arsenic adsorption isotherm studies follow the Langmuir model due to the higher numerical regression value. The value of R^2 related to arsenic adsorption by the studied nanosorbent was 0.995 for Langmuir isotherm and 0.8652 for Freundlich isotherm, which showed better compliance with the Langmuir isotherm. Freundlich and Langmuir isotherm models are used to model many adsorption processes. In the Langmuir isotherm, it is assumed that a single layer of adsorbate is

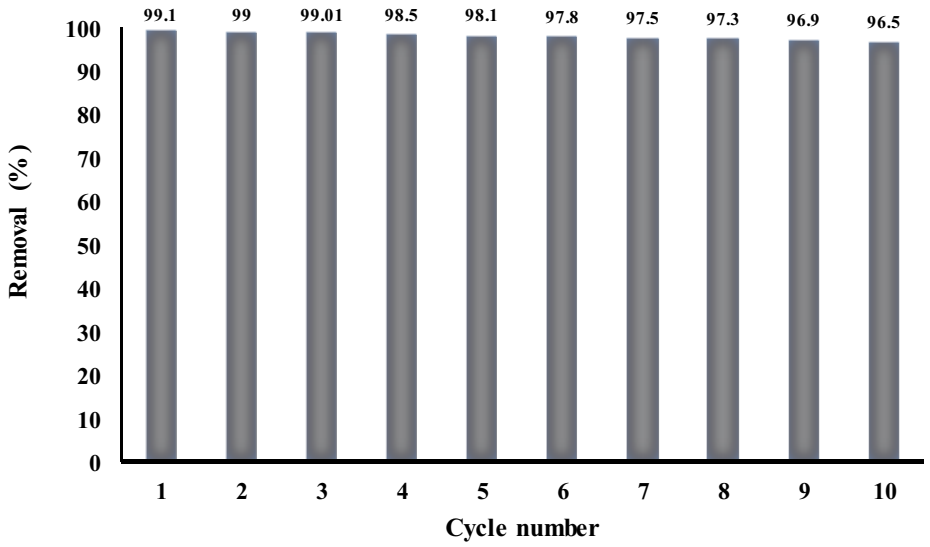

Fig. 8. Recyclability performance of the ACαZnO/TiO_2 nanoparticles for removal of arsenic.

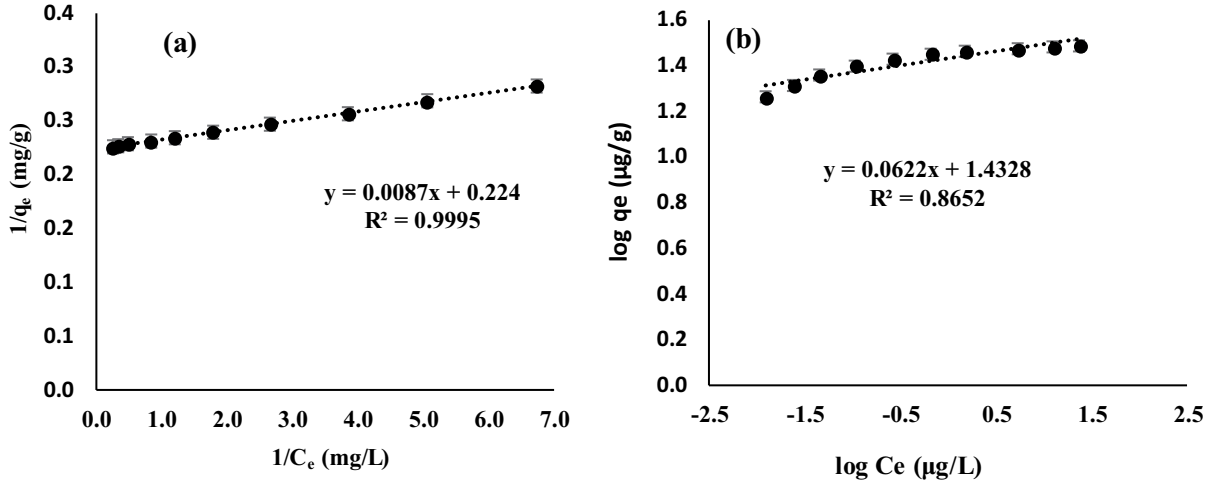

Fig. 9. (a) Langmuir and (b) Freundlich isotherm model for arsenic adsorption.

located on the homogeneous surface of the adsorbent, and the adsorption of each molecule on the surface has the same adsorption activation energy. In the Freundlich model, it is assumed that the adsorption of adsorbate on the surface of the adsorbent is heterogeneous adsorption and the energy of adsorption sites for the adsorbate is different from each other. The Langmuir equation is reliable for the process of adsorption on perfectly uniform surfaces, while the Freundlich equation is applicable for non-uniform surfaces [75].

Although the Langmuir isotherm represents the adsorption of many compounds on adsorbents, its assumptions are seldom correct because most adsorbents have defects (the adsorbent is not uniform), and the adsorbate molecules are usually not pure, so adsorption for initial molecules adsorbate and subsequent molecules are not the same. The Brunauer–Emmett–Teller model is very useful for eliminating the mentioned shortcomings [76]. A better fit of the Langmuir isotherm model indicates that a layer of the adsorbate component covers the adsorbent surface and the adsorption of each molecule of the adsorbate component has equal activation energy. It also indicates the homogeneity of the adsorbent. Following the adsorption process from the Langmuir isotherm model is indicative of this fact that the adsorption of the ionic substrate (cationic or anionic) faces weak competition from solvent molecules [76,77].

3.7.2. Kinetic studies

Kinetic models are proposed to clarify the adsorption mechanism and evaluate the adsorbent performance, which depends on the physical and chemical properties of the adsorbent and the mass transfer process. Adsorption kinetics of the adsorbate component is required to select the optimal process conditions on a large scale. Kinetic parameters that are useful for predicting adsorption rate provide important information for process design and modeling [78,79]. One of the most important factors in designing the adsorption

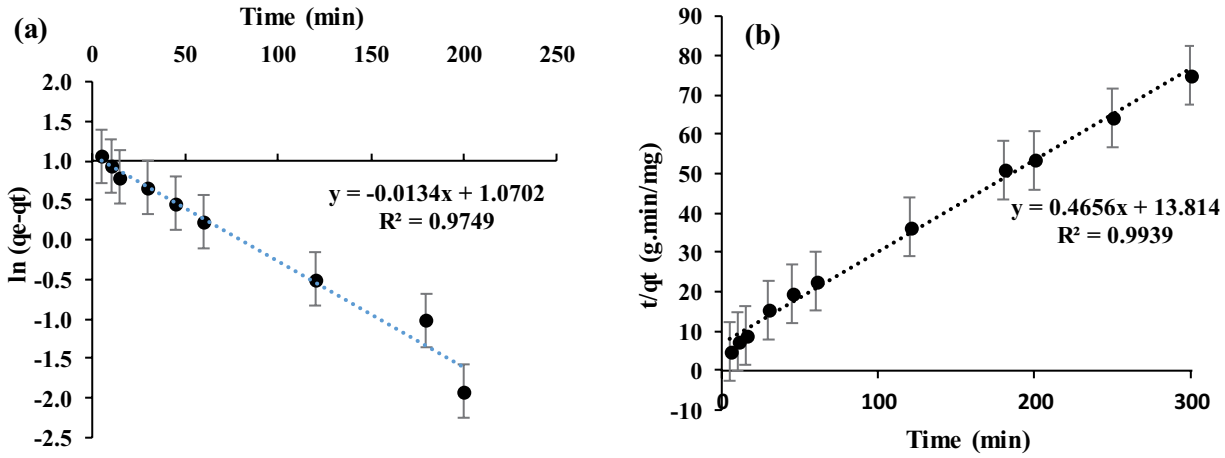

Fig. 10. (a) Pseudo-first kinetic model and (b) pseudo-second kinetic model for arsenic adsorption.

system (to determine the residence time of the adsorbate and the dimensions of the reactor) is the prediction of the rate of the adsorption process, which is controlled by the kinetics of the system. Adsorption kinetics depend on the physical and chemical properties of the adsorbent, which affects the adsorption mechanism [78–82]. Second-order reactions proceed at a rate commensurate with the square of raw material, while for first-order kinetics, the rate is proportional to the concentration of the contaminant. Pseudo-second kinetic shows that chemical adsorption is a rate-slowing step and controls adsorption processes [11,83,84]. According to Fig. 10, based on the comparison of the R^2 values obtained for the first and second order kinetics, it was shown that in the case of the modified adsorbent for arsenic adsorption, the results follow the pseudo-second-order model. Also, the adsorption capacity of arsenic and the isotherm model by other adsorbents are presented in Table 4.

4. Conclusion

The obtained experimental data were fitted to the quadratic model during CCD analysis, and the relationship between arsenic adsorption and independent factors was expressed using a quadratic polynomial equation. The results showed that the adsorption of arsenic on the adsorbent is well described by the pseudo-second kinetic model (R^2 > 0.99). The adsorption process follows the Langmuir isotherm model, which states the existence of monolayer adsorption (R^2 > 0.99). The results also showed that the optimal conditions for the studied parameters were as follows: pH = 6.75, arsenic concentration = 9.76 mg/L, reaction time = 287.62 min, and nanosorbent dose = 2.45 g/L. The maximum amount of arsenic adsorption under optimal conditions was predicted to be 4.53 mg/g. In general, the results of the study showed that the adsorption process can be used as an effective process in the adsorption of heavy metals such as arsenic from aqueous solutions.

Acknowledgment

This article is an extracted from the PhD thesis on Environmental Engineering. This work was supported by the Tehran North Branch, Islamic Azad University, Tehran, Iran.

References

[1] A. Dargahi, H. Golestanifar, P. Darvishi, A. Karami, S.H. Hasan, A. Poormohammadi, A. Behzadnia, An investigation and comparison of removing heavy metals (lead and chromium) from aqueous solutions using magnesium oxide nanoparticles, Pol. J. Environ. Stud., 25 (2016) 557–562.
[2] M. Farrokhi, M. Naimi-Joubani, A. Dargahi, M. Poursadeghiyan, H. Ali Jamali, Investigating activated sludge microbial population efficiency in heavy metals removal from compost leachate, Pol. J. Environ. Stud., 27 (2018) 623–627.
[3] A. Dargahi, H. Rahimzadeh, M. Vosoughi, S.A. Mokhtari, Enhanced electrocatalytic degradation of 2,4-Dinitrophenol (2,4-DNP) in three-dimensional sono-electrochemical (3D/SEC) process equipped with Fe/SBA-15 nanocomposite particle electrodes: degradation pathway and application for real wastewater, Arabian J. Chem., 15 (2022) 103801.
[4] S. Naseri, A.R. Mesdaghinia, A.H. Mahvi, M. Afsharnia, Recycling and reuse potential for effluents of metal and non-metal industries of Tehran metropolitan, Hakim J., 5 (2002) 20–31.
[5] M. Shams, N. Tavakkoli Nezhad, A. Dehghan, H. Alidadi, M. Paydar, A.A. Mohammadi, A. Zarei, Heavy metals exposure, carcinogenic and non-carcinogenic human health risks assessment of groundwater around mines in Joghatai, Iran, Int. J. Environ. Anal. Chem., (2020) 1–16, doi: 10.1080/03067319.2020.1743835.
[6] A. Dargahi, M. Vosoughi, S.A. Mokhtari, Y. Vaziri, M. Alighadri, Enhanced electrocatalytic degradation of 2,4-Dinitrophenol (2,4-DNP) in three-dimensional sono-electrochemical (3D/SEC) process equipped with Fe/SBA-15 nanocomposite particle electrodes: degradation pathway and application for real wastewater, Arabian J. Chem., 15 (2022) 103648.
[7] K. Sharafi, M. Pirsaheb, T. Khosravi, A. Dargahi, M. Moradi, M.T. Savadpour, Fluctuation of organic substances, solids, protozoan cysts, and parasite egg at different units of a wastewater integrated stabilization pond (full scale treatment plant): a case study, Iran, Desal. Water Treat., 57 (2016) 4913–4919.
[8] A. Almasi, A. Dargahi, M. Ahagh, H. Janjani, M. Mohammadi, L. Tabandeh, Efficiency of a constructed wetland in controlling organic pollutants, nitrogen, and heavy metals from sewage, J. Chem. Pharm. Sci., 9 (2016) 2924–2928.
[9] W.-W. Tang, G.-M. Zeng, J.-L. Gong, J. Liang, P. Xu, C. Zhang, B.-B. Huang, Impact of humic/fulvic acid on the removal of heavy metals from aqueous solutions using nanomaterials: a review, Sci. Total Environ., 468 (2014) 1014–1027.

[10] Z. Honarmandrad, N. Javid, M. Malakootian, Efficiency of ozonation process with calcium peroxide in removing heavy metals (Pb, Cu, Zn, Ni, Cd) from aqueous solutions, SN Appl. Sci., 2 (2020) 1–7.
[11] R. Askari, S. Afshin, Y. Rashtbari, A. Moharrami, F. Mohammadi, M. Vosuoghi, A. Dargahi, Synthesis of activated carbon from walnut wood and magnetized with cobalt ferrite ($CoFe_2O_4$) and its application in removal of cephalexin from aqueous solutions, J. Dispersion Sci. Technol., 18 (2021) 1–2.
[12] L. Tabandeh, G. Khorramabadi, A. Karami, Z. Atafar, H. Sharafi, A. Dargahi, F. Amirian, Evaluation of heavy metal contamination and scaling and corrosion potential in drinking water resources in Nurabad city of Lorestan, Iran, Int. J. Pharm. Technol., 8 (2016) 13137–13154.
[13] J.-f. Liu, Z.-s. Zhao, G.-b. Jiang, Coating Fe_3O_4 magnetic nanoparticles with humic acid for high efficient removal of heavy metals in water, Environ. Sci. Technol., 42 (2008) 6949–6954.
[14] X. Qu, P.J. Alvarez, Q. Li, Applications of nanotechnology in water and wastewater treatment, Water Res., 47 (2013) 3931–3946.
[15] S.R. Chowdhury, E.K. Yanful, Arsenic and chromium removal by mixed magnetite–maghemite nanoparticles and the effect of phosphate on removal, J. Environ. Manage., 91 (2010) 2238–2247.
[16] P. Pillai, S. Dharaskar, Zeolitic Imidazolate Framework-8 as promising nanoparticles for arsenic removal from aqueous solution, Int. J. Nanotechnol., 18 (2021) 414–426.
[17] G.K. Das, C.S. Bonifacio, J. De Rojas, K. Liu, K. Van Benthem, I.M. Kennedy, Ultra-long magnetic nanochains for highly efficient arsenic removal from water, J. Mater. Chem., 2 (2014) 12974–12981.
[18] A. Srivastava, K. Selvaraj, K.S. Prasad, Pollution, nanoparticles based adsorbent for removal of arsenic from aqueous solution, Asian J. Water Environ. Pollut., 16 (2019) 97–103.
[19] S.S. Bhargav, I. Prabha, Removal of arsenic and copper metals from contaminated water using iron(III) oxide nanoparticle, Int. J. Chem. Chem. Eng., 2 (2013) 107–112.
[20] D. De, S.M. Mandal, J. Bhattacharya, S. Ram, S.K. Roy, Iron oxide nanoparticle-assisted arsenic removal from aqueous system, J. Environ. Sci. Health A, 44 (2009) 155–162.
[21] Y. Babaee, C.N. Mulligan, M.S. Rahaman, Removal of arsenic(III) and arsenic(V) from aqueous solutions through adsorption by Fe/Cu nanoparticles, J. Chem. Technol. Biotechnol., 93 (2018) 63–71.
[22] S. Eybpoosh, N. Khanjani, Residual concentrations of arsenic and its health effects in the Iranian population: a systematic review, J. Health Dev., 4 (2015) 168–180.
[23] M. Bissen, F.H. Frimmel, Arsenic—a review. Part II: oxidation of arsenic and its removal in water treatment, Acta Hydrochim. Hydrobiol., 31 (2003) 97–107.
[24] S. Wickramasinghe, B. Han, J. Zimbron, Z. Shen, M. Karim, Arsenic removal by coagulation and filtration: comparison of groundwaters from the United States and Bangladesh, Desalination, 169 (2004) 231–244.
[25] M. Uddin, M. Mozumder, M. Islam, S. Deowan, J. Hoinkis, Nanofiltration membrane process for the removal of arsenic from drinking water, Chem. Eng. Technol., 30 (2007) 1248–1254.
[26] Y.-h. Xu, T. Nakajima, A. Ohki, Adsorption and removal of arsenic(V) from drinking water by aluminum-loaded Shirasu-zeolite, J. Hazard. Mater., 92 (2002) 275–287.
[27] V.M. Boddu, K. Abburi, J.L. Talbott, E.D. Smith, R. Haasch, Removal of arsenic(III) and arsenic(V) from aqueous medium using chitosan-coated biosorbent, Water Res., 42 (2008) 633–642.
[28] X. Zhang, K. Jiang, Z. Tian, W. Huang, L. Zhao, Removal of arsenic in water by an ion-exchange fiber with amino groups, J. Appl. Polym. Sci., 110 (2008) 3934–3940.
[29] M. Habuda-Stanić, M. Nujić, Arsenic removal by nanoparticles: a review, Environ. Sci. Pollut. Res., 22 (2015) 8094–8123.
[30] C.H. Nguyen, M.L. Tran, T.T. Van Tran, R.-S. Juang, Enhanced removal of various dyes from aqueous solutions by UV and simulated solar photocatalysis over TiO_2/ZnO/rGO composites, Sep. Purif. Technol., 232 (2020) 115962, doi: 10.1016/j.seppur.2019.115962.
[31] B. Sayan, S. Indranil, M. Aniruddha, C. Dhrubajyoti, C. Uday, C. Debashis, Role of nanotechnology in water treatment and purification: potential applications and implications, Int. J. Chem. Sci. Technol., 3 (2013) 59–64.
[32] A. Peyghami, A. Moharrami, Y. Rashtbari, S. Afshin, M. Vosuoghi, A. Dargahi, Evaluation of the efficiency of magnetized clinoptilolite zeolite with Fe_3O_4 nanoparticles on the removal of basic violet 16 (BV16) dye from aqueous solutions, J. Dispersion Sci. Technol., (2021) 1–10, doi: 10.1080/01932691.2021.1947847.
[33] A. Dargahi, M. Moradi, R. Marafat, M. Vosoughi, S.A. Mokhtari, K. Hasani, S.M. Asl, Applications of advanced oxidation processes (electro-Fenton and sono-electro-Fenton) for degradation of diazinon insecticide from aqueous solutions: optimization and modeling using RSM-CCD, influencing factors, evaluation of toxicity, and degradation pathway, Biomass Convers. Biorefin., (2021) 1–18, doi: 10.1007/s13399-021-01753-x.
[34] K. Hasani, M. Moradi, S.A. Mokhtari, A. Dargahi, M. Vosoughi, Degradation of basic violet 16 dye by electro-activated persulfate process from aqueous solutions and toxicity assessment using microorganisms: determination of by-products, reaction kinetic and optimization using Box–Behnken design, Int. J. Chem. React., 19 (2021) 261–275.
[35] A. Seidmohammadi, Y. Vaziri, A. Dargahi, H. Zolghadr Nasab, Improved degradation of metronidazole in a heterogeneous photo-Fenton oxidation system with PAC/Fe_3O_4 magnetic catalyst: biodegradability, catalyst specifications, process optimization, and degradation pathway, Biomass Convers. Biorefin., (2021) 1–7.
[36] V. Vaiano, G. Iervolino, D. Sannino, L. Rizzo, G. Sarno, A. Farina, Enhanced photocatalytic oxidation of arsenite to arsenate in water solutions by a new catalyst based on MoO_x supported on TiO_2, Appl. Catal., B, 160 (2014) 247–253.
[37] M. Gholami, M. Shirzad-Siboni, M. Farzadkia, J.-K. Yang, Synthesis, characterization, and application of ZnO/TiO_2 nanocomposite for photocatalysis of a herbicide (Bentazon), Desal. Water Treat., 57 (2016) 13632–13644.
[38] N. Javid, M. Malakootian, Removal of bisphenol A from aqueous solutions by modified-carbonized date pits by ZnO nanoparticles, Desal. Water Treat., 95 (2017) 144–151.
[39] K. Hasani, M. Moradi, A. Dargahi, M. Vosoughi, Evaluation of cefixime toxicity treated with sono-electro-Fenton process by bioassay using microorganisms, Avicenna J. Environ. Health Eng., 8 (2021) 22–27.
[40] M.H. Dehghani, A. Zarei, A. Mesdaghinia, R. Nabizadeh, M. Alimohammadi, M. Afsharnia, Response surface modeling, isotherm, thermodynamic and optimization study of arsenic(V) removal from aqueous solutions using modified bentonite-chitosan (MBC), Korean J. Chem. Eng., 34 (2017) 757–767.
[41] M. Darvishmotevalli, A. Zarei, M. Moradnia, M. Noorisepehr, H. Mohammadi, Optimization of saline wastewater treatment using electrochemical oxidation process: prediction by RSM method, MethodsX, 6 (2019) 1101–1113.
[42] M.H. Dehghani, R.R. Karri, Z.T. Yeganeh, A.H. Mahvi, H. Nourmoradi, M. Salari, A. Zarei, M. Sillanpää, Statistical modelling of endocrine disrupting compounds adsorption onto activated carbon prepared from wood using CCD-RSM and DE hybrid evolutionary optimization framework: comparison of linear vs non-linear isotherm and kinetic parameters, J. Mol. Liq., 302 (2020) 112526, doi: 10.1016/j.molliq.2020.112526.
[43] M.R. Samarghandi, A. Dargahi, A. Rahmani, A. Shabanloo, A. Ansari, D. Nematollahi, Application of a fluidized three-dimensional electrochemical reactor with Ti/SnO_2–Sb/β-PbO_2 anode and granular activated carbon particles for degradation and mineralization of 2,4-dichlorophenol: process optimization and degradation pathway, Chemosphere, 279 (2021) 130640, doi: 10.1016/j.chemosphere.2021.130640.
[44] S. Afshin, Y. Rashtbari, M. Vosough, A. Dargahi, M. Fazlzadeh, A. Behzad, M. Yousefi, Application of Box–Behnken design for optimizing parameters of hexavalent chromium removal from aqueous solutions using Fe_3O_4 loaded on activated carbon

prepared from alga: kinetics and equilibrium study, J. Water Process. Eng., 42 (2021) 102113, doi: 10.1016/j.jwpe.2021.102113.
[45] A. Dargahi, R. Shokoohi, G. Asgari, A. Ansari, D. Nematollahi, M.R. Samarghandi, Moving-bed biofilm reactor combined with three-dimensional electrochemical pretreatment (MBBR–3DE) for 2,4-D herbicide treatment: application for real wastewater, improvement of biodegradability, RSC Adv., 11 (2021) 9608–9620.
[46] A. Dargahi, M.R. Samarghandi, A. Shabanloo, M.M. Mahmoudi, H.Z. Nasab, Statistical modeling of phenolic compounds adsorption onto low-cost adsorbent prepared from aloe vera leaves wastes using CCD-RSM optimization: effect of parameters, isotherm, and kinetic studies, Biomass Convers. Biorefin., (2021) 1–15, doi: 10.1007/s13399-021-01601-y.
[47] M. Heidari, M. Vosoughi, H. Sadeghi, A. Dargahi, S.A. Mokhtari, Degradation of diazinon from aqueous solutions by electro-Fenton process: effect of operating parameters, intermediate identification, degradation pathway, and optimization using response surface methodology (RSM), Sep. Sci. Technol., 56 (2021) 2287–2299.
[48] K. Hasani, S. Hosseini, H. Gholizadeh, A. Dargahi, M. Vosoughi, Enhancing the efficiency of electrochemical, Fenton, and electro-Fenton processes using SS316 and SS316/β-PbO_2 anodes to remove oxytetracycline antibiotic from aquatic environments, Biomass Convers. Biorefin., (2021) 1–18
[49] S. Alavi, S. Shamshiri, Z. Pariz, A. Dargahi, M. Mohamadi, S. Fathi, T. Amirian, Evaluating the palm leaves efficiency as a natural adsorbent for removing cadmium from aqueous solutions: isotherm adsorption study, Int. J. Pharm. Technol., 8 (2016) 13919–13929.
[50] M. Mahmoodi Meimand, N. Javid, M. Malakootian, Adsorption of sulfur dioxide on clinoptilolite/nano iron oxide and natural clinoptilolite, Health Scope, 8 (2019) e69158.
[51] R. Shokoohi, R.A. Gillani, M.M. Mahmoudi, A. Dargahi, Investigation of the efficiency of heterogeneous Fenton-like process using modified magnetic nanoparticles with sodium alginate in removing Bisphenol A from aquatic environments: kinetic studies, Desal. Water Treat., 101 (2018) 185–192.
[52] A. Dargahi, K. Hasani, S.A. Mokhtari, M. Vosoughi, M. Moradi, Y. Vaziri, Highly effective degradation of 2,4-Dichlorophenoxyacetic acid herbicide in a three-dimensional sono-electro-Fenton (3D/SEF) system using powder activated carbon (PAC)/Fe_3O_4 as magnetic particle electrode, J. Environ. Chem. Eng., 9 (2021) 105889.
[53] M.M. Mahmoudi, S. Nasseri, A.H. Mahvi, A. Dargahi, M.S. Khubestani, M. Salari, Fluoride removal from aqueous solution by acid-treated clinoptilolite: isotherm and kinetic study, Desal. Water Treat., 146 (2019) 333–340.
[54] N. Javid, Z. Honarmandrad, M. Malakootian, Ciprofloxacin removal from aqueous solutions by ozonation with calcium peroxide, Desal. Water Treat., 174 (2020) 178–185.
[55] M.R. Samarghandi, G. Asgari, R. Shokoohi, A. Dargahi, A. Arabkouhsar, Removing amoxicillin antibiotic from aqueous solutions by Saccharomyces cerevisiae bioadsorbent: kinetic, thermodynamic and isotherm studies, Desal. Water Treat., 152 (2019) 306–315.
[56] M.R. Samarghandi, A. Ansari, A. Dargahi, A. Shabanloo, D. Nematollahi, M. Khazaei, H.Z. Nasab, Y. Vaziri, Enhanced electrocatalytic degradation of bisphenol A by graphite/β-PbO_2 anode in a three-dimensional electrochemical reactor, J. Environ. Chem. Eng., 9 (2021) 106072.
[57] A. Azizi, A. Dargahi, A. Almasi, Biological removal of diazinon in a moving bed biofilm reactor–process optimization with central composite design, Toxin Rev., 40 (2021) 1242–1252.
[58] M. Molla Mahmoudi, R. Khaghani, A. Dargahi, G. Monazami Tehrani, Electrochemical degradation of diazinon from aqueous media using graphite anode: effect of parameters, mineralisation, reaction kinetic, degradation pathway and optimisation using central composite design, Int. J. Environ. Anal. Chem., (2020) 1–26, doi: 10.1080/03067319.2020.1742893.
[59] A. Almasi, M. Mahmoudi, M. Mohammadi, A. Dargahi, H. Biglari, Optimizing biological treatment of petroleum industry wastewater in a facultative stabilization pond for simultaneous removal of carbon and phenol, Toxin Rev., 40 (2021) 189–197.
[60] M.O. Saeed, K. Azizli, M.H. Isa, M.J. Bashir, Application of CCD in RSM to obtain optimize treatment of POME using Fenton oxidation process, J. Water Process. Eng., 8 (2015) 7–16.
[61] S. Alizadeh, H. Sadeghi, M. Vosoughi, A. Dargahi, S.A. Mokhtari, Removal of humic acid from aqueous media using sono-persulphate process: optimization and modelling with response surface methodology (RSM), Int. J. Environ. Anal. Chem., (2020) 1–15, doi: 10.1080/03067319.2020.1772777.
[62] W. Ahmed, S. Mehmood, A. Núñez-Delgado, S. Ali, M. Qaswar, A. Shakoor, A.A. Maitlo, D.-Y. Chen, Adsorption of arsenic(III) from aqueous solution by a novel phosphorus-modified biochar obtained from *Taraxacum mongolicum* Hand-Mazz: adsorption behavior and mechanistic analysis, J. Environ. Manage., 292 (2021) 112764.
[63] H. Eisazadeh, A. Hemati, Adsorption of As(III) by using polythiophene/Fe_2O_3 nanocomposites synthesized in aqueous/non-aqueous media, J. Appl. Chem., 12 (2017) 139–156.
[64] A. Asgari, A. Mahvi, F. Vaezi, F. Khalili, Study of the efficiency of arsenic removal from drinking water by granular ferric hydroxide (GFH), QOM Univ. Med. Sci. J., 2 (2008) 53–65.
[65] K. Banerjee, S. Nour, M. Selbie, M. Prevost, C.D. Blumenschein, H. Chen, G.L. Amy, Optimization of Process Parameters for Arsenic Treatment with Granular Ferric Hydroxide, Proceedings of the AWWA Annual Conference, Anaheim, CA, USA, 2003, pp. 15–19.
[66] J. Sun, X. Zhang, A. Zhang, C. Liao, Preparation of Fe–Co based MOF-74 and its effective adsorption of arsenic from aqueous solution, J. Environ. Sci., 80 (2019) 197–207.
[67] Y. Zhang, M. Zhao, Q. Cheng, C. Wang, H. Li, X. Han, Z. Fan, G. Su, D. Pan, Z. Li, Research progress of adsorption and removal of heavy metals by chitosan and its derivatives: a review, Chemosphere, 279 (2021) 130927.
[68] M. Feng, P. Zhang, H.-C. Zhou, V.K. Sharma, Water-stable metal-organic frameworks for aqueous removal of heavy metals and radionuclides: a review, Chemosphere, 209 (2018) 783–800.
[69] G.K. Sarma, S. SenGupta, K.G. Bhattacharyya, Methylene blue adsorption on natural and modified clays, Sep. Sci. Technol., 46 (2011) 1602–1614.
[70] M.R. Sangi, A. Shahmoradi, J. Zolgharnein, G.H. Azimi, M. Ghorbandoost, Removal and recovery of heavy metals from aqueous solution using *Ulmus carpinifolia* and *Fraxinus excelsior* tree leaves, J. Hazard. Mater., 155 (2008) 513–522.
[71] P.S. Kumar, S. Ramalingam, K. Sathishkumar, Removal of methylene blue dye from aqueous solution by activated carbon prepared from cashew nut shell as a new low-cost adsorbent, Korean J. Chem. Eng., 28 (2011) 149–155.
[72] M. Mosaferi, A.R. Mesdaghinia, Removal of arsenic from drinking water using modified activated alumina, J. Water Wastewater, 55 (2005) 2–14.
[73] A. Bhatnagar, M. Sillanpää, Utilization of agro-industrial and municipal waste materials as potential adsorbents for water treatment—a review, Chem. Eng. J., 157 (2010) 277–296.
[74] A. Maleki, A. Eslami, Isotherm and kinetics of arsenic(V) adsorption from aqueous solution using modified wheat straw, Iran. J. Health Environ., 3 (2011) 439–450.
[75] A. Seidmohammadi, G. Asgari, A. Dargahi, M. Leili, Y. Vaziri, B. Hayati, A.A. Shekarchi, A. Mobarakian, A. Bagheri, S.B. Nazari Khanghah, A. Keshavarzpour, A comparative study for the removal of methylene blue dye from aqueous solution by novel activated carbon based adsorbents, Prog. Color Color Coat., 12 (2019) 133–144.
[76] R. Shokoohi, A. Dargahi, R.A. Gilan, H.Z. Nasab, D. Zeynalzadeh, M.M. Mahmoudi, Magnetic multi-walled carbon nanotube as effective adsorbent for ciprofloxacin (CIP) removal from aqueous solutions: isotherm and kinetics studies, Int. J. Chem. React., 18 (2020) 1–16.
[77] H. Celebi, I. Bilican, T. Bahadir, Applicability of innovative adsorbents in geogenic arsenic removal, J. Cleaner Prod., 327 (2021) 129475.

[78] M.R. Samarghandi, A. Dargahi, H. Zolghadr Nasab, E. Ghahramani, S. Salehi, Degradation of azo dye Acid Red 14 (AR14) from aqueous solution using H2O2/nZVI and $S_2O_8^{2-}$/nZVI processes in the presence of UV irradiation, Water Environ. Res., 92 (2020) 1173–1183.
[79] Y. Lee, Y. Ren, M. Cui, Y. Zhou, O. Kwon, J. Ko, J. Khim, Arsenic adsorption study in acid mine drainage using fixed bed column by novel beaded adsorbent, Chemosphere, 291 (2021) 132894, doi: 10.1016/j.chemosphere.2021.132894.
[80] A. Seid-Mohammadia, Z. Ghorbanianb, G. Asgaria, A. Dargahic, Photocatalytic degradation of metronidazole (MNZ) antibiotic in aqueous media using copper oxide nanoparticles activated by H, Desal. Water Treat., 193 (2020) 369–380.
[81] A. Othmani, S. Magdouli, P.S. Kumar, A. Kapoor, P.V. Chellam, Ö. Gökkuş, Agricultural waste materials for adsorptive removal of phenols, chromium(VI) and cadmium(II) from wastewater: a review, Environ. Res., 204 (2022) 111916.
[82] M. Samarghandi, A. Rahmani, G. Asgari, G. Ahmadidoost, A. Dargahi, Photocatalytic removal of cefazolin from aqueous solution by AC prepared from mango seed + ZnO under UV irradiation, Global Nest J., 20 (2018) 399–407.
[83] T.J. Al-Musawi, P. Rajiv, N. Mengelizadeh, I.A. Mohammed, D. Balarak, Development of sonophotocatalytic process for degradation of acid orange 7 dye by using titanium dioxide nanoparticles/graphene oxide nanocomposite as a catalyst, J. Environ. Manage., 292 (2021) 112777.
[84] A. Seid-Mohammadi, G. Asgarai, Z. Ghorbanian, A. Dargahi, The removal of cephalexin antibiotic in aqueous solutions by ultrasonic waves/hydrogen peroxide/nickel oxide nanoparticles (US/H_2O_2/NiO) hybrid process, Sep. Sci. Technol., 55 (2020) 1558–1568.